Characterization of brick and brick–mortar interface under uniaxial tension

VII International Seminar on Structural Masonry for Developing Countries

18th to 20th September 2002
Belo Horizonte, Brazil

J. C. Almeida[1], P. B. Lourenço[2], J. A. Barros[2]

[1] Instituto Piaget – ISEIT/VISEU
Estrada do Alto do Gaio –Lordosa – 3510-651 Viseu
e-mail: jcalmeida@viseu.ipiaget.pt

[2] Department of Civil Engineering, University of Minho
School of Engineering, University of Minho
P-4800-058 Guimarães, Portugal
e-mail: pbl@civil.uminho.pt; barros@civil.uminho.pt

ABSTRACT: *Softening is a gradual decrease of mechanical resistance under a continuous increase of deformation imposed on a material specimen or structure. It is a salient feature of quasi-brittle materials like clay brick, mortar, ceramics, rock or concrete, which fail due to a process of progressive internal crack growth. Such mechanical behavior is commonly attributed to the heterogeneity of the material, due to the presence of different phases and material defects, like flaws and voids. The initial stresses and cracks as well as variations of internal stiffness and strength cause progressive crack growth when the material is subjected to progressive deformation. Initially, the micro cracks are stable which means that they grow only when the load is increased. Around peak load an acceleration of crack formation takes place and the formation of macro cracks starts. The macro cracks are unstable, which means that the load has to decrease to avoid an uncontrolled growth. In a deformation controlled test the macro crack growth results in softening and localization of cracking in a small zone, while the rest of the specimen unloads.*

For tensile failure this phenomenon has been well identified for concrete but very few results exists for masonry. In the present paper, the results of an extensive set of tests, carried out at University of Minho, including brick specimens and masonry specimens under uniaxial tension will be presented. Both tensile strength and fracture energy are quantified, for different bricks and different types of brick-mortar interface.

Key words: Units, mortar-joints, softening, uniaxial tension.

1 INTRODUCTION

The objective of the present paper is to characterize the tensile behavior of units and unit-mortar interface, for different bricks and mortars used in Portugal and Spain.

In a tensile test of a quasi-brittle material, such as brick, it is possible to obtain a stress-elongation diagram σ-u in the form indicated in Fig. 1, provided that the test is carried out under displacement control.

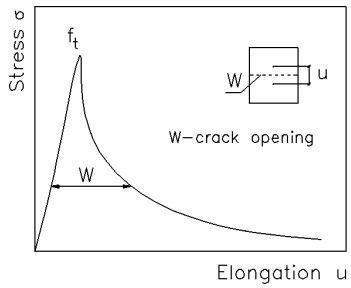

Fig. 1 – Stress-elongation diagram

The illustrated behavior indicates that, after reaching the peak load, the strength does not drop immediately to zero. Instead the strength is gradually reduced in a process denoted as "softening". The behavior up to peak can be considered linear, but after peak significant non-linearity is found in the response. According to Van Mier (1997), the post-peak behavior can assume two different shapes, as illustrated in Fig. 2, depending on the end restraints of the tested specimen.

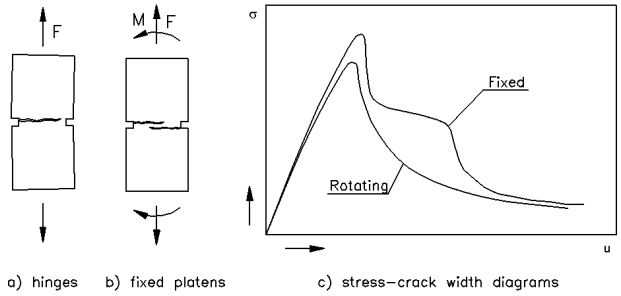

Fig. 2 – Rotating vs. fixed end restrains

The behavior in Fig. 2a (rotating platens or hinges) is justified by the rotation of the specimen during the loading operation, where the crack proceeds from one side of the specimen to the other side. In case of Fig. 2b, fixed (non-rotating) platens, a bending moment is introduced and multiple cracks will appear. This results in a slightly larger tensile strength and a higher value of energy dissipated (fracture energy).

The tensile strength of the constituents of masonry, namely units and mortar, is a key parameter for modern numerical modeling and for understanding the behavior of masonry structures.

In the present paper, the use of different tensile strength set-ups is addressed and a significant number of experimental results are shown for three types of ceramic bricks and four types of mortar.

2 TENSILE TESTS

Next, a brief summary of the methods to characterize the tensile strength of brick and mortar is given, see Jukes and Riddington (1998) for further details.

2.1 *Direct tensile bond strength test methods. Couplet tests*

This test consists of two units connected by only one mortar joint. It is the simplest specimen and, at the same time, the most economic, taking into account the number of bricks required. Nevertheless, to carry out deformation controlled tests, sophisticated low capacity universal testing machines are usually required.

A couplet test using special clamps was utilized by Palmer and Hall (1931), Polyakov (1956) and Jung (1988). This method, represented schematically in Fig. 3, includes the use of steel clamps, so that bolts are utilized to clamp the specimen.

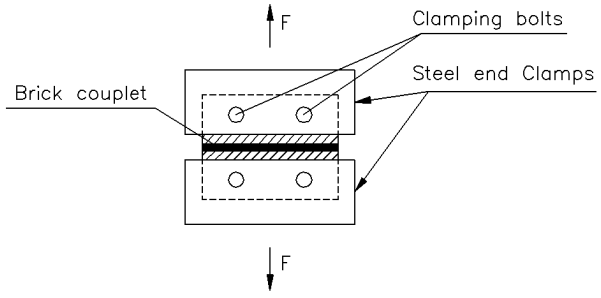

Fig. 3 – Couplet test using special clamps

A variation of this method is the one used by Ritchie (1961), which utilizes a series of five units of clay bricks and four mortar joints, see Fig. 4. No benefit seems to derive from this particular set-up.

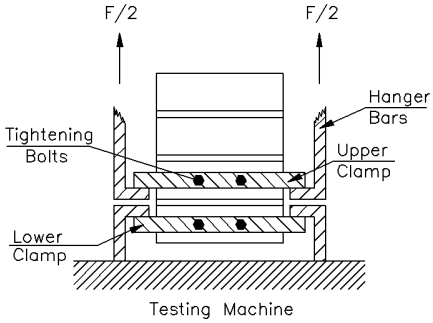

Fig. 4 – Couplet test using clamps

Another possibility is to use transverse holes and bolts, as illustrated in Fig. 5, and adopted by Murthy and Hendry (1965), Sinha and Hendry (1966), Ghazali (1986), and Jukes (1997). In this set-up, the load is applied by means of steel plates and transverse bolts. The bolts are inserted in brick cavities previously drilled in the specimens. Ideally, the holes are localized at a distance equal to one quarter of the brick length from the extremities and at half of the height of the brick.

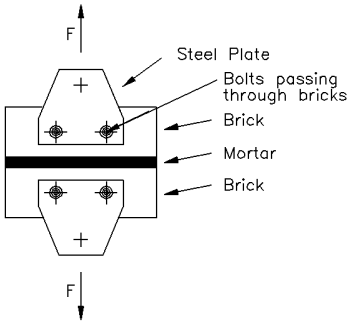

Fig. 5 – Couplet test using holes and bolts

A different loading arrangement was developed by Taylor-Firth and Taylor (1990), allowing to test the specimen without the need to use clamping devices to hold the bricks. The load is applied by means of tie bars placed under the bricks, as shown in Fig 6.

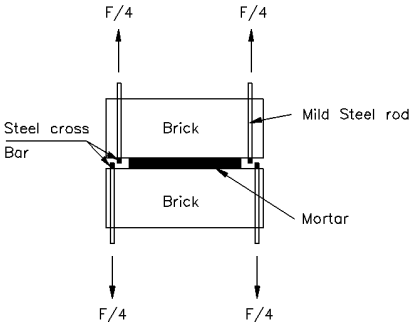

Fig. 6 – Sheffield test

Finally, another possibility is to glue the unit against the steel end plates using epoxy resin. Several authors adopted this procedure: Van Der Pluijm (1993), Kuenning (1966), Sinha and Hendry (1975), Chinwah (1972), Ghazali (1986). For this set-up, load is applied to the specimen by means of plates that are bonded with an adhesive as it is shown in Fig 7.

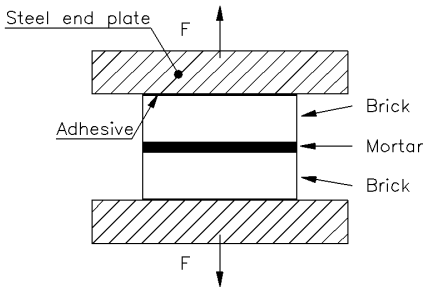

Fig. 7 – Steel plates glued with adhesive

It is noted that Van Der Pluijm (1993) adopted the variant shown in Fig. 8 and obtained the post-peak characteristic of the response, being the sole author able to trace the complete response of the material. Noteworthy, the net bond area in his specimens was only about 35% of the total area of the joint due to deficient curing conditions in the outside the joint.

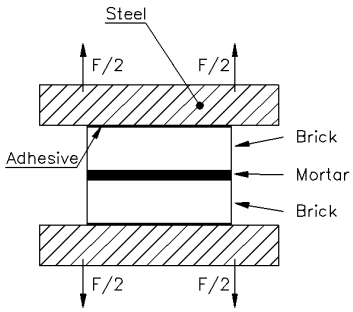

Fig. 8 – Steel and plates glued with adhesive, Van der Pluijm (1993)

2.2 *Crossed brick couplet*

A different test, with very minor equipment requirements was proposed in 1976. This type of test, included in the American Standard C952-76 (1976), is performed by applying compressive loads in the upright bars as it is shown in Fig 9.

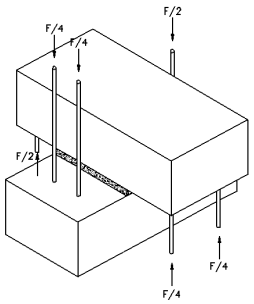

Fig. 9 – Crossed brick couplet

2.3 *Bending Tests*

A relatively easy test to carry out is the three-point or four-point loading test, so that the flexural bond strength can be obtained. It is noted that the flexural bond strength depends on the height of the specimen and low insight is available with respect to the relationship between masonry flexural bond strength and tensile bond strength.

For this reason, direct tension tests (with epoxy-glued specimen ends) should be preferred.

3 MATERIALS

3.1 *Bricks*

Tensile tests were performed with solid (S) bricks, hollow bricks produced in Portugal (HP), and hollow bricks produced in Spain (HS). Each clay brick was tested in vertical (V) and in horizontal (H) direction resulting in six series with the following notation: SV, SH; HPV, HPH; HSV, HSH. Table 1 gives the dimensions of the brick specimens and the free water absorption measured.

Table 1. Series of brick specimens

Bricks	Dimensions [mm]	Free water absorption [mass-%]
S	$220 \times 110 \times$	9.7
HP	$220 \times 110 \times$	10.6
HS	$240 \times 100 \times$	14.6

Notched specimens are required to perform uniaxial tensile deformation controlled tests in homogenous materials. In an attempt to ensure stable tests, the notch where the controller displacement was applied had a depth higher than the notch at the opposite side. The ratio between the depths of these two notches was not kept constant, but the area of the real crack surface (between notches) was measured to evaluate the stress applied. Both notches had 3 mm width.

Grooves were introduced on the brick end surfaces to increase the bond of the specimen to the machine platens.

3.1.1 *S Bricks*

This type of brick is current on the market and has the dimensions of $220 \times 100 \times 70$ mm^3. Due to the maximum load bearing capacity (25 kN), and the space available between the platens of the testing machine (90 mm), $40 \times 40 \times 70$ mm^3 S brick specimens were extracted according to the scheme shown in Fig. 10.

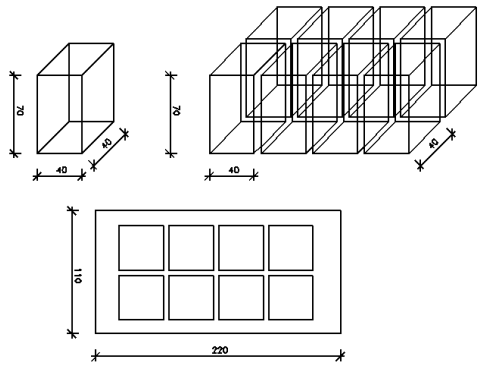

Fig. 10 – SV Units

3.1.2 *HP Bricks*

To increase the bonding of HP brick specimens to the machine loading platens, the brick end surfaces were grooved. Fig. 11 shows the dimensions of the two types of HP specimens extracted from the bricks, being representative of the brick shell and web.

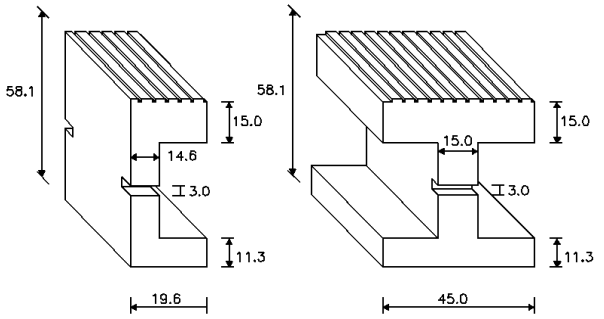

(a) (b)

Fig. 11 – HPV Units: Specimens for (a) brick shell and (b) brick web

3.1.3 *HS Bricks*

This brick has four horizontal holes and a rough surface on the top surface. Fig. 12 shows the specimens adopted to characterize the shell and web of the brick, respectively, to the left and right of the figure.

Fig. 12 – Specimens for HSH Units

3.2 *Mortar*

Four different types of mortars were adopted for the 10 mm thick joint, changing the proportions, in weight, of the (binder):sand, namely: (1):3, (1):4, (1):5 and (1:2):9. In the first three mixes, Portland cement class normal 32.5 was used, featuring a compressive strength of 32.5 N/mm^2 at 28 days (according to Norm NP EN 196-1, 1990). In the last mix, the binder was made using 1/3 of this cement and 2/3 of hydrated lime. In all mixes, the same natural sand was used, with the following grading (percent of retained material, in weight): sieve #30, 51.3%; sieve #50, 17.0%; sieve #100, 4.5%; sieve #200, 1.8%.

Bending and compression tests were carried out, according to Norm NP EN 196(1990), to characterize the mortars. The results obtained are given in Table 2.

Table 2. Mortar properties

Mortar	Flexural strength	Compression strength
	$f_{ct,f}$ (N/mm^2)	f_c (/mm^2)
1:3	4.3	12.8
1:4	3.3	10.9
1:5	1.9	7.1
1:2:9	2.2	6.4

4 TESTING EQUIPEMENT AND APPLIED MEASURING DEVICES

The tensile tests were performed in the laboratory of the Civil Engineering Department of University of Minho, using a CS 7400 – S shearing testing equipment. This machine has two independent hydraulic actuators, positioned in vertical and horizontal directions.

Since three-dimensional non-uniform crack opening can occur on tensile tests, Hordijk (1991), the tensile test control using the average signal of the deformations registered on the four corners of the specimen is the most appropriate procedure, see Fig. 13. However, the available equipment can only control one displacement transducer (LVDT). Therefore, the controller transducer was placed at half height of one saw-cut surface, and another LVDT was positioned on the same place of the opposite surface (see Fig. 14). These transducers have a measure base of 1 mm with a linearity of 0.17% of the full stroke. A deformation rate of 0.5 μm/s was used in the tests. The force applied was measured on a load cell of 25kN maximum load bearing capacity, with an accuracy of 0.03%.

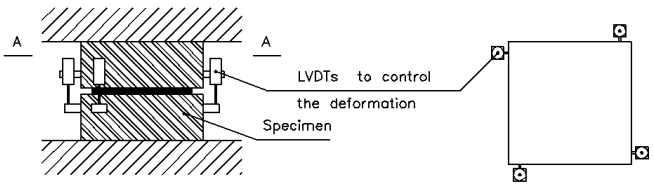

Fig. 13 – Position of LVDTs

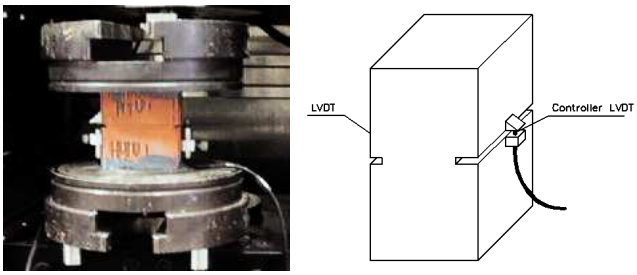

Fig. 14 – Brick specimens

5 RESULTS AND DISCUSSION

5.1 *Introduction*

From the force-elongation relationship obtained on the tensile tests, the following parameters were evaluated: tensile strength, fracture energy and residual stress at ultimate scan reading.

The results obtained by Van Der Pluijm (1999) revealed that the saw cuts reduce the Young's modulus of the brick (E_b) around 20% – 40%. For this reason, an estimation of E_b is not shown here.

Fig. 15 represents the procedure adopted for evaluating the fracture energy, G_f. The stress was determined dividing the force by the fracture surface (surface between notches).

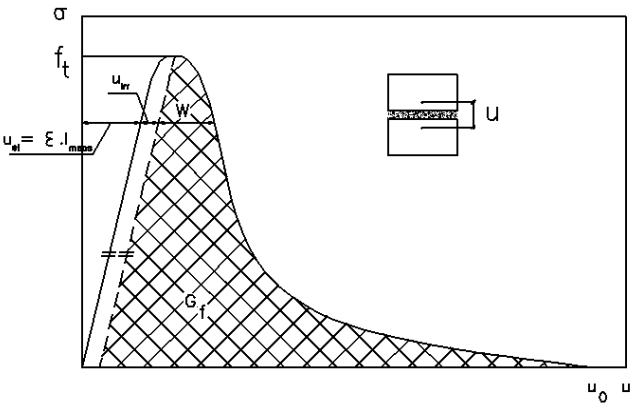

Fig. 15 – Schematic representation of the procedure to evaluate the fracture energy, G_f

Analyzing the force-deflection relationship obtained in stable tests (see Figs. 16-21), it was possible to verify that the descending branch approaches the horizontal axis gradually. In addition, the testing equipment has internal friction. Taking into account these two aspects, the fracture energy was evaluated up to a deflection of 60 μm or up to a deflection corresponding to a force of 200 N (if it is less than 60 μm). For the tests aborted before these limit conditions, the energy dissipated was not evaluated.

5.2 *Bricks*

5.2.1 *HS specimens*

Figs. 16 and 17 show the stress-elongation relationships recorded on HSV and HSH brick specimens, respectively. Tables 3 and 4 include the values of the main parameters evaluated for these two series of brick specimens. Analyzing the data, it is possible to observe a considerable scatter on the tensile strength, on the fracture energy and on the shape of the softening branch. For the specimens with higher strength, larger stress decay after peak load has occurred. The descending curves of some specimens, sometimes, displayed irregularities, which are due to the non-uniform crack opening, as it was already reported by other researchers, Hordijk (1991).

In the HSV series, 22% of the specimens have failed before attaining the ultimate deformation condition, while in the HSH series this number has increased for 50%. This is most likely due to the orientation of the cracks developed during drying and firing the bricks. In the remainder specimens the test was interrupted for an elongation of 60 μm, when the tensile strength was between 0.2 to 0.5 MPa.

Comparing the data obtained in the two series, it was observed that fracture energy is similar in the two directions, but HSH specimens showed a tensile strength 39% higher, due to the extrusion process.

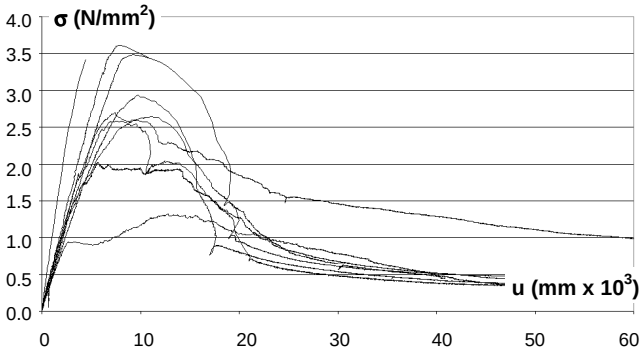

Fig. 16 – Stress-elongation on HSV brick specimens

Table 3. Results on HSV brick specimens

Unit	f_t [N/mm^2]	f_{tu} [N/mm^2]	f_{tu}/f_t [-]	$G_{f,meas}$ [N/mm]
HSV$_1$	3.43	3.43	100%	-
HSV$_3$	2.58	0.45	17%	0.04747
HSV$_4$	2.69	0.69	33%	0.09196
HSV$_6$	1.32	0.33	25%	0.03629
HSV$_7$	2.64	0.33	15%	0.05634
HSV$_8$	3.61	3.45	95%	-
HSV$_9$	3.48	0.40	15%	0.06948
HSV$_{10}$	2.93	0.33	15%	0.05275
HSV$_{12}$	2.02	0.33	16%	0.04681
Mean	**2.75**			**0.05730**
CV	**27%**			**32%**

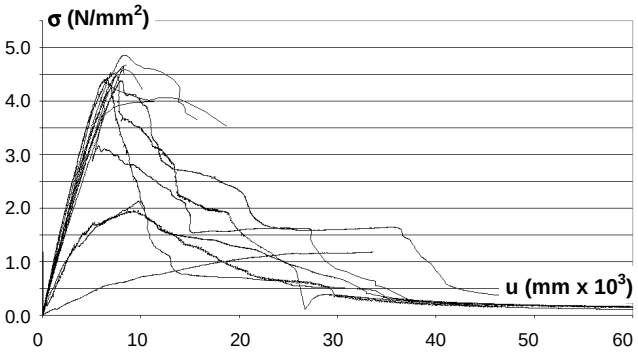

Fig. 17 – Stress-elongation on HSH brick specimens

Table 4. Results on HSH brick specimens

Unit	f_t [N/mm^2]	f_{tu} [N/mm^2]	f_{tu}/f_t [-]	$G_{fl,meas}$ [N/mm]
HSH $_1$	4.44	0.16	4%	0.05449
HSH$_2$	4.58	4.21	92%	-
HSH $_2$	4.64	4.49	97%	-
HSH $_3$	2.14	0.11	5%	0.03249
HSH $_5$	4.13	0.09	2%	0.06507
HSH $_6$	4.68	4.68	100%	-
HSH $_7$	3.99	3.99	100%	-
HSH $_9$	4.86	3.65	75%	-
HSH$_{10}$	4.38	0.22	5%	0.09347
HSH$_{11}$	1.18	1.18	100%	-
HSH$_{12}$	4.26	3.53	83%	-
HSH$_{13}$	4.48	0.14	3%	0.06297
HSH$_{14}$	1.97	0.15	8%	0.03402
Mean	**3.82**			**0.05708**
CV	**32%**			**40%**

5.2.2 *HP specimens*

Figs. 18 and 19 show the stress-elongation relationships obtained on HPV and HPH specimens, respectively. The main data evaluated are included on Tables 5 and 6. Similar to the HS specimens, the tensile strength of HP specimens, loaded horizontally, was higher than the values obtained in the HP specimens loaded vertically (increase of 51%). HPH specimens have developed a fracture energy 53% higher than the one evaluated on HPV specimens.

In HP specimens the scatter of the data registered was significantly higher than the results determined on HS specimens, mainly the tensile strength, which might be related to the manufacturing process (an old plant, with non-uniform firing temperature, was adopted for manufacturing these bricks). In spite of this, HP specimens have developed tensile strength higher than HS specimens. HPV and HSV have shown similar capacity for dissipating fracture energy, but HPH specimens had high-energy absorption capacity than HSH.

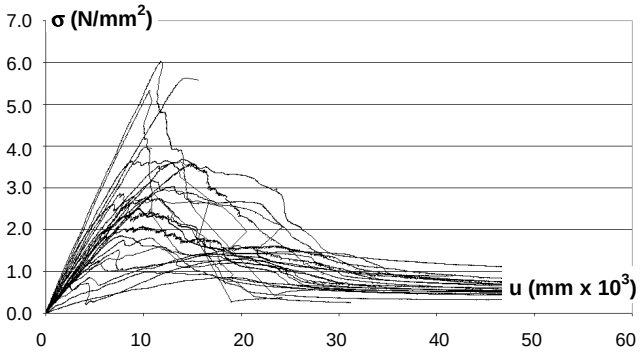

Fig. 18 – Stress-elongation on HPV brick specimens

Table 5. Results on HPV brick specimens

Unit	f_t [N/mm^2]	f_{tu} [N/mm^2]	f_{tu}/f_t [-]	$G_{fl,meas}$ [N/mm]
HPV$_1$	3.59	0.53	15%	0.06214
HPV$_2$	2.65	0.59	22%	0.06334
HPV$_3$	3.98	3.93	99%	-
HPV$_4$	1.00	0.26	26%	0.01294
HPV$_5$	3.17	0.89	28%	0.06741
HPV$_6$	3.62	3.36	93%	-
HPV$_7$	5.63	5.58	99%	-
HPV$_8$	1.85	0.33	18%	0.02553
HPV$_9$	2.52	0.52	21%	0.05567
HPV$_{10}$	1.28	0.66	52%	0.02305
HPV$_{11}$	2.50	0.52	21%	0.05533
HPV$_{12}$	1.81	0.42	23%	0.04511
HPV$_{13}$	1.49	0.63	43%	0.04671
HPV$_{14}$	1.59	0.57	36%	0.05476
HPV$_{15}$	2.95	0.53	18%	0.08582
HPV$_{16}$	1.52	0.47	31%	0.06064
HPV$_{17}$	2.87	0.53	19%	0.06088
HPV$_{18}$	1.32	0.47	36%	0.04133
HPV$_{19}$	0.86	0.41	48%	0.02721
HPV$_{20}$	2.09	0.63	30%	0.06885
HPV$_{21}$	2.74	0.59	22%	0.07582
HPV$_{22}$	3.60	0.45	13%	0.07586
HPV$_{23}$	2.80	0.37	13%	0.02108
HPV$_{24}$	6.03	0.45	8%	0.07885
HPV$_{25}$	3.69	0.63	17%	0.10657
HPV$_{26}$	4.81	4.64	96%	-
HPV$_{27}$	5.33	0.48	9%	0.06530
Mean	**2.86**			**0.05566**
CV	**49%**			**41%**

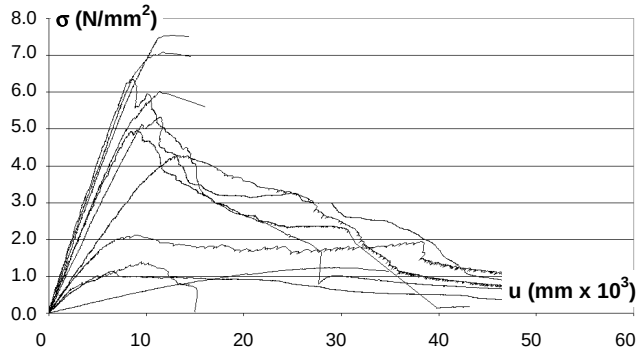

Fig. 19 – Stress-elongation on HPH brick specimens

Table 6. Results on HPH brick specimens

Unit	f_t [N/mm^2]	f_{tu} [N/mm^2]	f_{tu}/f_t [-]	$G_{fl,meas}$ [N/mm]
HPH_1	1.14	0.19	16%	0.03722
HPH_2	4.97	0.18	4%	0.09794
HPH_3	2.12	0.42	20%	0.08562
HPH_4	4.28	0.38	9%	0.11637
HPH_5	1.24	1.14	92%	-
HPH_3	6.03	5.61	93%	-
HPH_4	1.41	0.03	2%	0.01217
HPH_5	7.54	7.50	100%	-
HPH_6	7.09	6.97	98%	-
HPH_7	5.32	0.31	6%	0.13136
HPH_8	6.36	0.39	6%	0.11609
Mean	**4.32**			**0.08525**
CV	**57%**			**52%**

5.2.3 *S specimens*

The stress-elongation relationships for specimens SV and SH are depicted on Figs. 20 and 21, respectively. The main data evaluated is included on Tables 7 and 8. The SV series had a tensile strength 18% higher and fracture energy 15% higher than the values obtained on SH series. Like in previous series, the scatter on the S series was also too high, particularly, on the tensile strength of SH series. After testing, internal cracks and voids in some bricks were observed, justifying the obtained scatter. The tensile strength and the fracture energy of S series were of the same order of the HS and HP series.

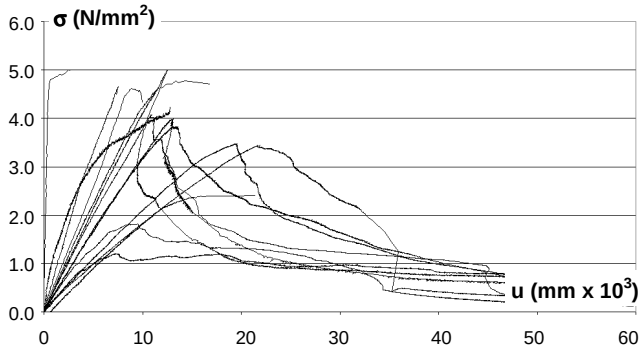

Fig. 20 – Stress-elongation on SV brick specimens

Table 7. Results on SV specimens

Unit	f_t [N/mm^2]	f_{tu} [N/mm^2]	f_{tu}/f_t [-]	$G_{fl,meas}$ [N/mm]
SV_1	1.21	0.20	17%	0.05460
SV_2	3.83	3.70	97%	-
SV_3	3.48	0.19	5%	0.08083
SV_4	3.45	0.25	7%	0.04285
SV_5	0.84	0.51	60%	0.02842
SV_6	0.89	0.16	18%	0.02580
SV_7	1.82	0.12	7%	0.04307
SV_9	5.00	4.99	100%	-
SV_{10}	4.62	4.33	94%	-
SV_{13}	3.83	0.28	7%	0.09179
SV_{14}	4.66	4.48	96%	-
SV_{17}	4.08	0.23	6%	0.07864
SV_{19}	4.23	4.21	99%	-
SV_{22}	5.00	0.72	14%	0.06075
SV_{23}	4.78	4.71	99%	-
SV_{24}	3.99	0.11	3%	0.06861
Mean	**3.48**			**0.05754**
CV	**42%**			**39%**

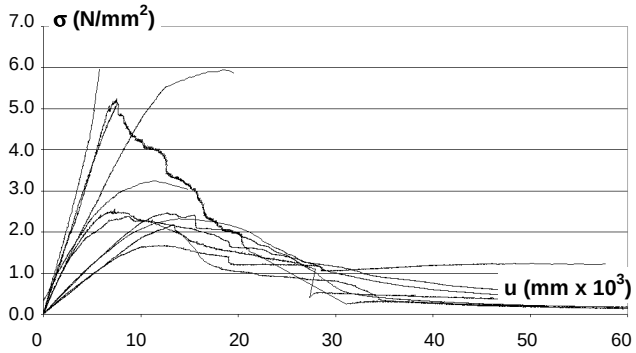

Fig. 21 – Stress-elongation on SH brick specimens

Table 8. Results on SH specimens

Units	f_t [N/mm^2]	f_{tu} [N/mm^2]	f_{tu}/f_t [-]	$G_{fl,meas}$ [N/mm]
SH_1	2.47	0.15	6%	0.05227
SH_2	1.68	1.22	73%	0.06045
SH_3	2.32	0.40	17%	0.06638
SH_4	0.69	0.24	35%	-
SH_6	0.80	0.16	21%	0.00954
SH_7	0.81	0.18	22%	0.03051
SH_8	2.18	0.16	7%	0.03961
SH_9	2.56	0.29	11%	0.05784
SH_{10}	5.97	5.97	100%	-
SH_{13}	5.09	5.02	99%	-
SH_{15}	2.38	0.17	7%	0.06029
SH_{17}	5.95	5.87	99%	-
SH_{18}	3.24	3.04	94%	-
SH_{19}	5.25	0.12	2%	0.07656
Mean	**2.96**			**0.05083**
CV	**63%**			**41%**

5.3 *Solid brick-mortar interface specimens*

Fig.s 22 to 24 illustrate the stress-elongation relationships for specimens composed by two halves of SV bricks connected by the type of mortars described on Section 3.2. The main data evaluated is included on Tables 9 to 11.

These tests were rather instable and the softening branch could be obtained only in a few tests. The values of the fracture energy and the tensile strength were lower that the values registered on the brick-only specimens. The highest tensile strength was found on specimens with a 1:4 mortar joint.

The results of the specimens with a 1:5 mortar joint are not presented, because their load bearing capacity was negligible.

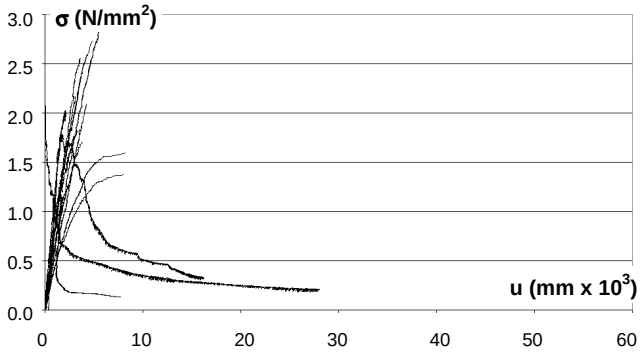

Fig. 22 – Stress-elongation on specimens SV-1:3 mortar

Table 9. Results on specimens SV-1:3 mortar

Unit	f_t [N/mm^2]	f_{tu} [N/mm^2]	f_{tu}/f_t [-]	$G_{fl,meas}$ [N/mm]
M_1	2.77	2.77	100%	-
M_2	2.01	2.01	100%	-
M_3	2.17	2.17	100%	-
M_4	1.70	1.70	100%	-
M_7	2.03	2.00	99%	-
M_9	1.15	0.13	12%	0.00167
M_{10}	2.10	0.21	10%	0.01062
M_{11}	1.37	1.37	100%	-
M_{12}	2.56	2.54	99%	-
M_{13}	2.09	2.09	100%	-
M_{14}	2.73	2.73	100%	-
M_{15}	1.78	0.33	18%	0.01209
M_{16}	2.84	2.83	100%	-
M_{17}	1.59	1.59	100%	-
Mean	**2.06**			**0.00813**
CV	**25%**			**69%**

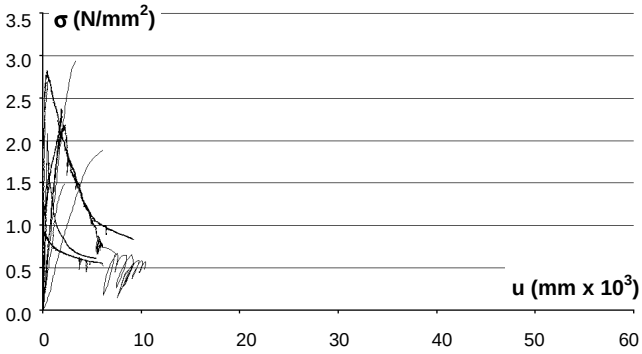

Fig. 23 – Stress-elongation on specimens SV-1:4 mortar.

Table 10. Results on specimens SV-1:4 mortar

Unit	f_t [N/mm^2]	f_{tu} [N/mm^2]	f_{tu}/f_t [-]	$G_{fl,meas}$ [N/mm]
M_{18}	2.82	0.837	30%	0.01290
M_{19}	2.75	2.747	100%	-
M_{21}	1.90	1.896	100%	-
M_{22}	2.94	2.944	100%	-
M_{27}	2.19	0.491	22%	0.01065
M_{28}	2.08	0.609	29%	0.00459
M_{30}	1.50	1.495	100%	-
M_{31}	2.37	0.513	22%	0.00302
M_{32}	1.74	1.739	100%	-
Mean	**2.25**			**0.00779**
CV	**22%**			**61%**

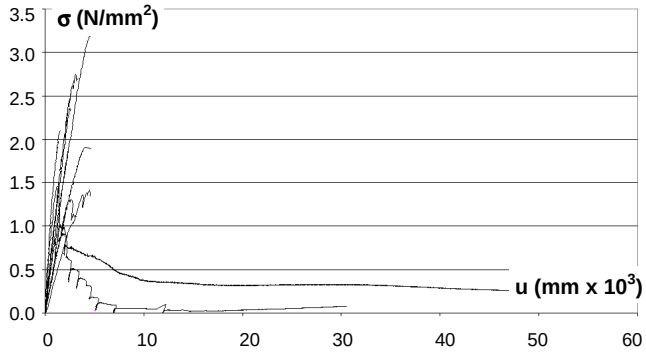

Fig. 24 – Stress-elongation on specimens SV-1:2:9 mortar

Table 11. Results on specimens SV-1:2:9 mortar

Unit	f_t [N/mm^2]	f_{tu} [N/mm^2]	f_{tu}/f_t [-]	$G_{fl,meas}$ [N/mm]
M_{33}	2.75	2.70	98%	-
M_{34}	0.91	0.08	9%	0.0234
M_{35}	1.46	0.19	13%	-
M_{36}	2.11	2.11	100%	-
M_{39}	2.35	2.32	99%	-
M_{40}	1.41	1.34	95%	-
M_{43}	1.31	1.10	84%	-
M_{45}	1.89	1.65	87%	-
M_{46}	3.19	3.19	100%	-
M_{47}	1.91	1.89	99%	-
Mean	**1.93**			**-**
CV	**36%**			**-**

6 CONCLUSIONS

The present paper aims at characterizing the tensile behavior of hollow bricks produced in Portugal (HP), hollow bricks produced in Spain (HS), solid bricks produced in Portugal (S) and brick-mortar interface. Three different producers have provided the bricks.

To accomplish this purpose, tensile tests on a servo-controlled machine were carried out. The results were obtained under controlled displacement, in order to obtain, not only the tensile strength, but also the shape of the softening branch and the energy dissipated up to a very low residual strength (fracture energy).

Two types of specimens were extracted from the hollow bricks, so that the shell and the web can be characterized. All bricks were tested in vertical (V) and horizontal (H) direction.

Due to the brittle behavior of clay brick units, in a significant number of specimens it was not possible to evaluate the fracture energy, since the test was interrupted before attained the deformation limit considered reasonable for assuming that the energy dissipated on cracking process was consumed.

In some tests, the softening branches have shown irregularities, typical of the three-dimensional non-uniform crack opening phenomenon. To avoid these local instabilities the uniaxial tensile tests would be better controlled by the average signal registered on 4 LVDTs placed on the edges of the brick specimens.

Due to the difficulties of assuring material and geometric homogeneity amongst brick specimens, a large scatter on the tensile strength and fracture energy was obtained. This scatter is typical of masonry materials under tension, see Van Der Pluijm (1999).

The results in the brick specimens are rather constant, if one takes into consideration that three different brick manufacturers have been considered. An average value of the tensile strength in the order of 3 N/mm^2 was obtained. In general, higher strength seems to be obtained in the extrusion direction even if S series results are difficult to understand due to the extremely large scatter. The series of brick specimens have developed average fracture energy values between 0.0512 and 0.081N/mm, the lowest average value was registered on SH series and the highest one on HPH series.

Due to the straight bond crack between brick and mortar, the post peak behavior could be tracked only in a very few specimens. In these specimens the average bond tensile strength was in the order of 2 N/mm^2 and the average fracture energy was extremely low (around 0.008 N/mm). It is noted the value of the interface fracture energy is around one tenth of the brick fracture energy. No significant differences were found with respect to the different mortar mixes (1:3, 1:4 and 1:2:9), with the exception of mortar mix 1:5 that resulted in (too weak) non measurable bond.

It is noted that the bond strength values obtained in the present paper are higher that in some literature, see e.g. Van Der Pluijm (1999). The reason for this difference seems to be related to the process of preparing the specimens. Here, the specimens were cast in groups of sixteen, pressed between two moulds so that a mortar thickness of 10 mm is found and, finally, the individual specimens were separated while the mortar was fresh. As a result, the actual bond area obtained in the present testing program was almost the full specimen. On the contrary, in Van Der Pluijm (1999) the actual bonding area was only 35% of the specimen cross section.

7 ACKNOWLEDGMENTS

The present work was partially supported by GROWTH project GROW-1999-70420 “ISO-BRICK” funded by European Commission.

8 REFERENCES

ASTM C-67 Standard Test Methods for Sampling and Testing Brick and Structural Clay Tile.

American Society For Testing And Materials. Test of bond strength of mortar to masonry units. ASTM C952/76, 1976.

Chinwah, J.C.G. Shear resistance masonry walls, Ph.D. thesis, Univ. London, 1972.

Ghazali, M.Z. Shear strength of brick masonry joints, D.Phil thesis, Univ. Sussex, 1986.

Hordijk, D.A. Local approach to fatigue of concrete, PhD Thesis, Technical University of Delft, Netherlands, 1991.

Jukes, P. An investigation into the shear strength of masonry joints, D.Phil thesis Univ. Sussex, 1997.

Jukes, P. and Riddington, J.R., A Review of Masonry Tensile Bond Strength Test Methods, Masonry International, Vol 12, nº2, 1998.

Jung, E. The binding between mortar and brick, Proc. SIBMAC. Ed.J.W.de Courey. London, Elsevier Applied Science, Conf., Dublin, Ireland, 182-193, 1988.

Kuenning, W.H. Improved method testing tensile bond strength of masonry mortars, J. of Materials, 1, (1), 180, 1966.

Murthy, C.K. and Hendry, A.W. Preliminary investigation of the shear strength of one-sixth scale model brickwork, Stoke-on-Trent, B. Ceram, R.A., TN65, Part 1, 1965.

NP EN196-1 Methods for testing cement (in Portuguese) (1990).

Palmer, L.A. and Hall, J.V. Durability and strength of bond between mortar and brick. Bur. Stand. J. Res., RP290, 6, 473, 1931.

Polyakov, S.V. Masonry in framed buildings, Moscow, Trans. G.L. Cairns, National Lending Library, Boston Spa. 1956.

Ritchie, T. A small-panel method for investigating moisture penetration and bond strength of brick masonry, Mat. Res. at Stand., 1, (5), 360, 1961.

Sinha, B.P. and Hendry, A.W. Further investigations of bond tension, bond shear and the effect of precompression on shear strength of model brick masonry couplets. Stoke-on-Trent, B. Ceram. R.A., TN80, 1966.

Sinha, B.P. and Hendry, A.W. Tensile strength of brickwork specimens, Proc. Brit. Ceram. Soc., Nº.24, Ed. H.W.H. We Stoke-on-Trent, N91, 1975.

Taylor-Firth, A. and Taylor, I.F. A bond tensile strength test for use in assessing the compatibility of brick/mortar interface Constr. and Build. Mat. 4, (2), 58-63, 1990.

Van Der Pluijm, R., Shear behavior of bed joints. Proc. 6th North Amer. Mas. Conf., Philadelphia, 125-136. 1993.

Van Der Pluijm, R., Out-of-plane Bending of Masonry Behavior and Strength, PhD Thesis, Eindhoven University of Technology, 1999.

Van Mier, Fracture Processes of Concrete, CRC Press, New York, 1997.